Decay Channel Dependence of the Photoelectron Angular Distributions in Core-Level Ionization of Ne Dimers

Masakazu Yamazaki,[1] Jun-ichi Adachi,[1] Yasuyuki Kimura,[1] Akira Yagishita,[1,*] Mauro Stener,[2,3,4] Piero Decleva,[2,3,4] Nobuhiro Kosugi,[5] Hiroshi Iwayama,[6] Kiyonobu Nagaya,[6] and Makoto Yao[6]

[1]*Photon Factory, Institute of Materials Structure Science, KEK, Oho 1-1, Tsukuba 305-0801, Japan*
[2]*Dipartimento di Scienze Chimiche, Università di Trieste, Via L. Giorgieri 1, I-34127 Trieste, Italy*
[3]*Consorzio Interuniversitario Nazionale per la Scienza e Tecnologia dei Materiali, Unitá di Trieste, Trieste, Italy*
[4]*INFM DEMOCRITOS, National Simulation Center, Trieste, Italy*
[5]*Institute for Molecular Science, Myodaiji, Okazaki 444-8585, Japan*
[6]*Department of Physics, Graduate School of Science, Kyoto University, Kyoto 606-8502, Japan*
(Received 4 February 2008; published 25 July 2008)

For K-shell photoionization of neon dimers, we report Ne 1s photoelectron angular distributions for $Ne^{2+} + Ne^{+}$ and $Ne^{+} + Ne^{+}$ channels exhibiting quite different patterns. Noninversion-symmetric patterns of the former obtained by the fast interatomic Coulombic decay of Auger final states show direct evidence of core-hole localization. Dipolar patterns of the latter obtained by the slow radiative decay of the other Auger final states clearly show that the radiative process is slow enough to allow dicationic dimers to rotate many times before fragmentation.

DOI: 10.1103/PhysRevLett.101.043004 PACS numbers: 33.80.Eh, 33.90.+h

According to chemical bonding theory, the valence electrons can be delocalized to form a chemical bond, and the core electrons are completely localized on each atom. Therefore, it is considered that the core hole created by x-ray absorption is localized even in symmetric molecules. However, according to quantum theory, the core-hole states of the symmetric molecules are degenerate to satisfy the symmetry requirements; i.e., the symmetry-adapted core-hole states are constructed using symmetrized combinations of the localized core-hole states. Although this is often called core-hole delocalization, the symmetry restoration in the orbital picture is not related to the core-hole delocalization [1]. In such symmetry-adapted representations, a question arises whether or not the core hole should be considered localized on one specific atomic center. One can argue that a simple answer to the question does not exist due to the fact that the selection of the appropriate physical representation depends on the scheme of measurements [2]. That is, if one specific atom having the core hole can be distinguished from the measurements, the measured parameters are described by the localized core-hole states, and if not, they are described by the symmetry-adapted core-hole states. The core-orbital photoionization process of Ne dimers (Ne_2) provides an ideal showcase to resolve the elusive fundamental problem, because both removal of a 1s electron and successive Auger decay are essentially of atomic nature in the van der Waals molecules [3]. In this Letter, we report Ne 1s photoelectron angular distributions (PADs) from Ne_2 in coincidence with Ne^{2+} and Ne^{+} ions produced via interatomic Coulombic decay (ICD) [3–10] of Auger final states and PAD in coincidence with Ne^{+} and Ne^{+} ions via radiative decay [11,12] of the other Auger final states.

The experiment has been conducted at the undulator beam line BL-2C [13] of the Photon Factory using a multi-coincidence velocity-map imaging spectrometer [14]. Ne dimers were produced by expanding Ne gas cooled to 83 K through a 50-μm-diameter orifice at a stagnation pressure of $\sim$1 atm [15]. The photon beam crossed perpendicularly with the supersonic jet of the Ne dimers from a skimmer. Electrons and ions were extracted by a uniform electrostatic field on opposite sides towards two position- and time-sensitive detectors with delay-line readout [16], and were detected in coincidence. The ion momenta were determined from the times of flight and impact positions on the detector. The projection of the electron momenta on the coplanar plane, which is defined by the electric vector and propagation direction of incident light, was determined from the positions. Figure 1 shows the correlation diagram of the electron energy (E_e) and kinetic energy release (KER) of the fragment ions, measured in coincidence with (a) Ne^{2+} and Ne^{+} ions and (b) two Ne^{+} ions. The E_e distributions were obtained by peeling the projection images of electrons. For the $Ne^{2+} + Ne^{+}$ channel, the island at $E_e = 10$ eV corresponds to the Ne 1s photoelectrons, whose energy is independent of the KER. In addition, prominent diagonal structures due to the ICD electrons [3] are observed and are denoted as ICD1 and ICD2. For the $Ne^{+} + Ne^{+}$ channel, only the island corresponding to the photoelectrons was observed. The weak diagonal line in $E_e < 2$ eV is due to the ICD electrons following Ne 2s photoionization [6]. In order to elucidate the interplay between the photoemission dynamics and fragmentation pathways, the triple coincidence signals of Ne^{+}, Ne^{+} (or Ne^{2+}), and Ne 1s photoelectrons were analyzed to obtain the vector correlations between them.

Figure 2 shows polar plots of the Ne 1s PADs relative to the dissociation axis of (a) $Ne^{2+} + Ne^{+}$ and (b) $Ne^{+} + Ne^{+}$ breakup channels along with our results of calculations. The laboratory-frame PADs (LF-PADs) of Ne_2,

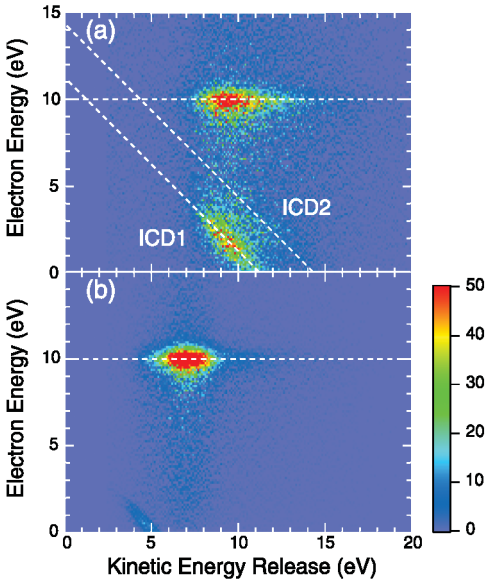

FIG. 1 (color). Correlation diagram between electron energy and kinetic energy release (KER) in fragmentation into (a) Ne^{2+} and Ne^{+} ions and (b) Ne^{+} and Ne^{+} ions. The color coding shows the relative electron intensities in arbitrary units. The photon energy was tuned to be 880.2 eV, just 10 eV above the Ne 1s ionization potential.

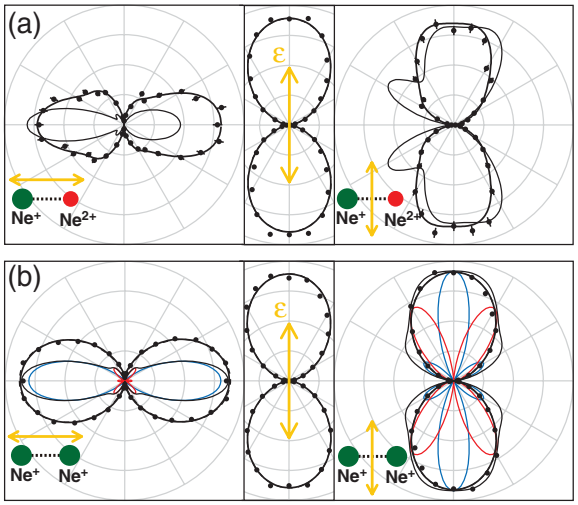

FIG. 2 (color). Polar plots of the Ne 1s PADs from Ne_2 in coincidence with (a) $Ne^{2+} + Ne^{+}$ and with (b) $Ne^{+} + Ne^{+}$ fragments at 10 eV photoelectron energy. The polarization vector ($\boldsymbol{\varepsilon}$) of the incident light and the dissociation direction of ion pairs are indicated. Filled circles with statistical error bars: experimental data; thick curves: fitting to data by Legendre polynomials up to tenth order, or by $[1 + \beta P_2(\cos\theta)]$; thin (black) curves: localized (a) and delocalized (b) theoretical MF-PADs which are normalized at the maximum data. In (b) $1\sigma_g^{-1}$ (blue) and $1\sigma_u^{-1}$ (red) components of MF-PADs are shown. Theoretical LF-PADs (broken curves) are hardly seen due to the overlap with fitting curves (see text).

which were obtained by integrating the PADs over all the back-to-back directions of the ion pairs, are also shown in the center. The systematic errors of each coincident PAD can be evaluated from the deviation of the data points of the LF-PAD from the dipolar pattern expressed by the fitted curve. They are comparable to the statistical errors of the data points. In the calculations, we employed the time-dependent density functional theory (TDDFT) described in Ref. [17], using the LB94 exchange-correlation potential with the ground-state density. The calculations were conducted using both localized and delocalized descriptions of the core-hole states. The molecular-frame PADs (MF-PADs) for the localized core hole are shown by thin curves in Fig. 2(a), where the photoelectron is ejected from the right Ne atom. The MF-PADs for the delocalized core-hole state with σ_g symmetry are shown by blue curves in Fig. 2(b) where the photoelectron is ejected coherently from both left and right Ne atoms, while those with σ_u are shown by red curves. The superposition of the two MF-PADs for σ_g and σ_u components is shown with thin black curves in Fig. 2(b) which is identical to the superposition of the two MF-PADs for the localized core holes on the left and right Ne atoms. The asymmetry parameter β for the LF-PAD was also calculated. As can be seen in Fig. 2(a), the PADs for the $Ne^{2+} + Ne^{+}$ channel depend on the mutual angle between the polarization vector and dissociation axis. Surprisingly, broken inversion symmetry of the PAD is seen clearly in the parallel geometry beyond the statistical errors of the data points, although the symmetry breaking is little recognized in the perpendicular. This observation implies that the atomic site of primary photoemission is recorded in the coincident PADs and that the fragmentation process is fast. As a consequence, the PADs result in the "MF-PADs." On the other hand, the PADs for the $Ne^{+} + Ne^{+}$ channel depend only on the polarization vector, and they are almost identical to the "LF-PADs." This implies that the dissociation direction of two Ne^{+} has no correlation with the dimer axis at the instant of the Ne 1s photoionization. Thus, the PADs shown in Fig. 2 demonstrate an intriguing new phenomenon on the relaxation of the core hole; the $Ne^{2+} + Ne^{+}$ channel retains the memory of both the molecular orientation and the initial core-hole localization, while both are lost in the $Ne^{+} + Ne^{+}$ channel.

In weakly bound van der Waals dimers, both a 1s photoemission and subsequent Auger decay with the lifetime of 2.4 fs [18] take place at one site. On this basis, the decay process of core ionized Ne_2 can be described by a two-step model: in the first step the Auger decay occurs at the initial core-hole site leading to $[Ne^{2+} - Ne]$, and in the second step a charge separation into two sites takes place during successive decays. As can be seen in the diagonal structures in Fig. 1(a), the ICD in the second step produces the Ne^{2+} and Ne^{+} ion pair. Since the Ne^{+} fragment arises from the neutral atom of $[Ne^{2+} - Ne]$ due to the ICD, one can presume that the initial core-hole memory was carried by the resultant fragment Ne^{2+} ion. Moreover, the lifetime of the order of 100 fs [3] of the ICD for $[Ne^{2+} - Ne]$ is much faster than the rotational period of about 100 ps

estimated from the ground-state molecular constant of $B_0 = 0.1553$ cm^{-1} [19]. Therefore, we conclude with certainty that the PADs for the $Ne^{2+} + Ne^{+}$ channel result in the MF-PADs, which shows noninversion-symmetric patterns reflecting symmetry lowering of the core ionized $[Ne^{+} - Ne]$. It should be noted here that the MF-PAD pattern is controlled by the interference between the direct and scattered photoelectron waves, which depends on electron energies and the mutual angle between the polarization vector and dimer axis. Therefore, the degree of core-hole localization is not directly related to the degree of the lack of inversion symmetry in the MF-PAD. For instance, the lack of inversion symmetry in the left MF-PAD in Fig. 2(a) reflects the strong influence of the scattered wave, in contrast to the right MF-PAD which is nearly inversion-symmetric and hardly affected by the scattered wave; nevertheless, the degree of core-hole localization does not depend on the geometries. The theoretical MF-PADs with the core hole localized on the Ne^{2+} site exhibit the lack of inversion symmetry; however, their patterns differ from the experimental ones in both the parallel and perpendicular geometries. The discrepancy is puzzling because our TDDFT calculations of the MF-PAD for other molecules [20–22] agree with the experimental results overall except for the shape resonance region. Moreover, the theoretical LF-PAD with the β of 1.88 well reproduces the experimental LF-PAD with the β of 1.92 ± 0.05 in the center of Fig. 2(a). A possible reason for the discrepancy might be the existence of the resonance because the coupling of photoemission with electronic decays and the coupling of it with nuclear motions, which were not included in the calculations, play an important role in the resonance [23]. The other possible reason, especially for the discrepancy of the favorite direction of photoemission in the parallel geometry, might come from the ambiguity on the observation of the core-hole position. That is, in the time-dependent picture of the core-hole state [24,25], the core hole is hopping from the Ne^{2+} to Ne in the Auger final states. The period of the hopping time can be estimated as ~690 fs, assuming that the *gerade* and *ungerade* energy separation in the Auger final state is comparable to that (6 meV [26]) in the inner-valence ionized states. Then, an appreciable portion of the initial core hole can move from the Ne^{2+} to Ne before the ICD, which was not taken into account in the calculations.

The PADs for the symmetric charge separation channel of $Ne^{+} + Ne^{+}$ ought to be inversion symmetric because the detection of such ions cannot distinguish the Ne atoms. In fact, the experimental PADs are inversion symmetric [see Fig. 2(b)], like the Ne 2*s* PAD from Ne_2 measured in coincidence with two Ne^{+} ions [26]. However, an essential difference between them exists. The present Ne 1*s* PAD does not depend on the dimer axis at all, which results in a LF-PAD; however, the Ne 2*s* PAD depends on the axis, which results in a MF-PAD. In the two-step model, a possible second step of fragmentation pathway to $Ne^{+} + Ne^{+}$ from the Auger final $[Ne^{2+}(^1D{:}2p^{-2}) + Ne]$ state is a radiative decay, as is the case of Ar_2 [11,12] because the Auger final state is energetically lower than the triply ionized state and cannot give off its excess energy by electron emission. During a lifetime (approximately nanoseconds) of the radiative decay leading to the symmetric charge separation, the dicationic dimer can rotate many times with a period of about 100 ps. Therefore, the memory of the molecular axis at the instant of photoionization is perfectly lost in the Ne 1*s* PAD. As a consequence, the observed coincident PADs are not MF-PADs but LF-PADs. Actually, the observed PADs are well explained by the theoretical LF-PAD. That is, the experimental β values determined from the PADs are 1.72 ± 0.02 and 1.85 ± 0.03 for the parallel and perpendicular geometry, respectively, and the theoretical β is 1.88, which is also in good agreement with the experimental β values, 1.85 ± 0.03 determined from the LF-PAD in the center of Fig. 2(b). This good agreement certainly supports the idea that the coincident PADs for the $Ne^{+} + Ne^{+}$ channel are reduced to the LF-PAD.

Hereafter, we rationalize the fragmentation pathways with the help of relevant potential energy curves of Ne_2 shown in Fig. 3. The theoretical method was an all-electron *ab initio* Hartree-Fock single-reference approach considering Ne 2*s* and 2*p* holes, explicitly using the GSCF3 code [27–29]. The basis functions used were Ne(4111111/31111/1*1*) and Ne(31111111/31111/1*1*) obtained from the contracted Gaussian-type function [73/7] as proposed by Huzinaga *et al.* [32]. The *d*-type polarization functions used were $\zeta = 0.852$ and 4.55. The van der Waals interaction was considered by the second-order Møller-Plesset many-body perturbation theory for a single reference configuration. The diagonal structures in Fig. 1(a) show that the sum of the KER and ICD electron energy is a constant. The energy (E_e + KER) of the ICD1 is about 11 eV. This value agrees with the energy difference (11.2 eV) between $[Ne^{2+}\ (^1P{:}2s^{-1}2p^{-1})$; 98.5 eV + Ne] and $[Ne^{2+}\ (^1D{:}2p^{-2})$; 65.7 eV + Ne^{+} $(2p^{-1})$; 21.6 eV]. The experimental value of the KER (~9 eV) agrees with the KER (~9.2 eV) estimated from the potential curve in Fig. 3 at the equilibrium distance (~3.1 Å) of the neutral Ne_2. One can also notice the weak diagonal structure (ICD2) for the sum energy of about 14 eV. This agrees with the energy difference (14.3 eV) between $[Ne^{2+}\ (^1P : 2s^{-1}2p^{-1})$; 98.5 eV + Ne] and $[Ne^{2+}\ (^3P{:}2p^{-2})$; 62.6 eV + Ne^{+} $(2p^{-1})$; 21.6 eV].

For the $Ne^{+} + Ne^{+}$ fragmentations, the most dominant radiative decay channel is indicated in Fig. 3. From the potential energy curves and the observed KER, significant bond shortening during the long lifetime can be recognized; the observed KER (~7 eV) of the $Ne^{+} + Ne^{+}$ pairs leads to the consequence that the radiative decay occurs around $R \sim 2$ Å. This is in accord with the equilibrium distance (~2.2 Å) of the $[Ne^{2+} - Ne]$ and is much shorter than that (3.1 Å) of the neutral ground state Ne_2 in contrast to the innervalence ionization, in which the fast ICD

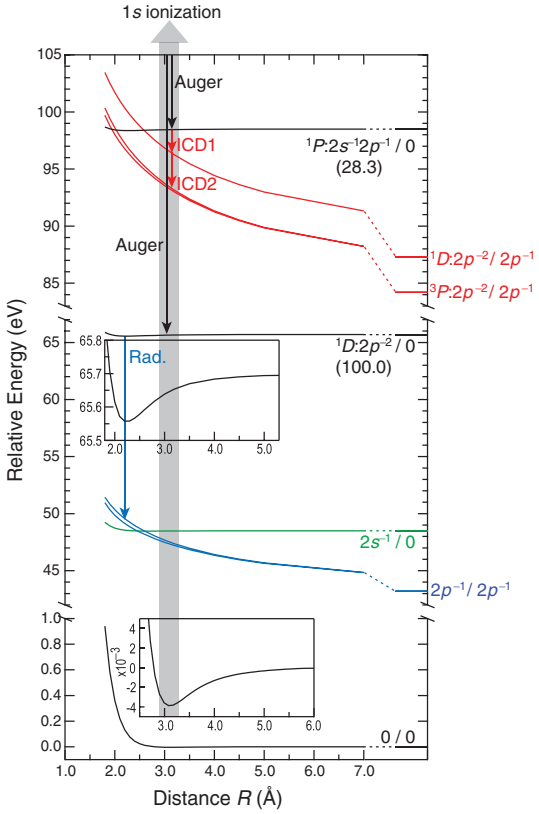

FIG. 3 (color). Calculated potential energy curves for the singly, doubly, and triply ionized states of Ne_2. At each dissociation limit, holes on each Ne atom are explicitly indicated, in which 0 represents the neutral electronic configuration. Potential curves are shifted according to the corresponding ionization energies [30,31] at the separated-atom limit. The dominant Auger final states are shown with the relative intensities [30] in parentheses.

process occurs at the equilibrium distance of the ground state Ne_2 resulting in the KER of ~4.5 eV [6,10].

In conclusion, we have demonstrated the Ne 1*s* PADs for $Ne^{2+} + Ne^+$ and $Ne^+ + Ne^+$ channels of van der Waals Ne dimers. The former containing the fast ICD, equivalent to MF-PAD, has given direct evidence of core-hole localization. The latter containing the slow radiative decay has lost the memory of molecular axis perfectly, and has been reduced to a LF-PAD. The present data of the MF-PAD provides a guide for further theoretical developments which may include the nuclear motion, core-hole relaxation, and channel mixing. Our findings on the deep-core ionization of the simplest cluster provide not only better understanding on the core-hole localization but also key fundamental information on core ionization and subsequent relaxation processes of more complex cluster systems and larger molecules, over the rather wide time scale ranging from femtoseconds to nanoseconds because there are no reasons to suppose our findings to be restricted to Ne_2 dimers.

The experiments have been performed under the approval of the Photon Factory Program Advisory Committee (Projects No. 2005G108 and No. 2007G056). We are grateful for valuable discussion with Professor L. S. Cederbaum. The present work was supported by a Grant-in-Aid for Scientific Research from the Japanese Ministry of Education, Culture, Sports, Science and Technology. M. Y. is grateful for the support of the JSPS.

Note added in proof.—When this manuscript was close to completion, we became aware of a paper considering a similar system [33].

*akira.yagishita@kek.jp

[1] N. Kosugi, Chem. Phys. **289**, 117 (2003).
[2] F. Gel'mukhanov and H. Ågren, JETP Lett. **67**, 1064 (1998).
[3] R. Santra and L. S. Cederbaum, Phys. Rev. Lett. **90**, 153401 (2003).
[4] L. S. Cederbaum, J. Zobeley, and F. Tarantelli, Phys. Rev. Lett. **79**, 4778 (1997).
[5] S. Marburger *et al.*, Phys. Rev. Lett. **90**, 203401 (2003).
[6] T. Jahnke *et al.*, Phys. Rev. Lett. **93**, 163401 (2004).
[7] G. Öhrwall *et al.*, Phys. Rev. Lett. **93**, 173401 (2004).
[8] Y. Morishita *et al.*, Phys. Rev. Lett. **96**, 243402 (2006).
[9] T. Aoto *et al.*, Phys. Rev. Lett. **97**, 243401 (2006).
[10] T. Jahnke *et al.*, Phys. Rev. Lett. **99**, 153401 (2007).
[11] R. Johnsen and M. A. Biondi, Phys. Rev. A **18**, 996 (1978).
[12] N. Saito *et al.*, Chem. Phys. Lett. **441**, 16 (2007).
[13] M. Watanabe *et al.*, Proc. SPIE Int. Soc. Opt. Eng. **3150**, 58 (1997).
[14] K. Hosaka *et al.*, Jpn. J. Appl. Phys. **45**, 1841 (2006).
[15] H. Murakami *et al.*, J. Chem. Phys. **126**, 054306 (2007).
[16] R. Dörner *et al.*, Phys. Rep. **330**, 95 (2000).
[17] M. Stener, G. Fronzoni, and P. Decleva, J. Chem. Phys. **122**, 234301 (2005).
[18] S. Svensson *et al.*, Phys. Scr. **14**, 141 (1976).
[19] A. Wüest and F. Merkt, J. Chem. Phys. **118**, 8807 (2003).
[20] M. Stener, Chem. Phys. Lett. **356**, 153 (2002).
[21] J. Adachi *et al.*, J. Phys. B **40**, 29 (2007).
[22] T. Teramoto *et al.*, J. Phys. B **40**, 4033 (2007).
[23] J. Adachi *et al.*, Phys. Rev. Lett. **91**, 163001 (2003).
[24] M. Tronc, G. C. King, and F. H. Read, J. Phys. B **12**, 137 (1979).
[25] J. Adachi *et al.*, J. Phys. B **40**, F285 (2007).
[26] T. Jahnke *et al.*, J. Phys. B **40**, 2597 (2007).
[27] N. Kosugi and H. Kuroda, Chem. Phys. Lett. **74**, 490 (1980).
[28] N. Kosugi, Theor. Chim. Acta **72**, 149 (1987).
[29] It is difficult to get well-balanced potential energy curves among states with different numbers of electrons due to slow convergence of dynamical electron correlation; therefore, we shifted each potential energy curve to fit its dissociation limit to experimental data [30,31].
[30] A. Albiez *et al.*, Z. Phys. D **16**, 97 (1990).
[31] ChE. Moore, *Ionization Potentials and Ionization Limits Derived from the Analyses of Optical Spectra* (U.S. GPO, Washington, DC, 1970).
[32] S. Huzinaga *et al.*, *Gaussian Basis Sets for Molecular Calculations* (Elsevier, Amsterdam, 1984).
[33] K. Kreidi *et al.*, J. Phys. B **41**, 101002 (2008).